APPLIED AND ENVIRONMENTAL MICROBIOLOGY, Jan. 2004, p. 363–369 Vol. 70, No. 1
0099-2240/04/$08.00+0 DOI: 10.1128/AEM.70.1.363–369.2004

Saturable, Energy-Dependent Uptake of Phenanthrene in Aqueous Phase by *Mycobacterium* sp. Strain RJGII-135

Naoyuki Miyata,[1]* Keisuke Iwahori,[1] Julia M. Foght,[2] and Murray R. Gray[3]

Institute for Environmental Sciences, University of Shizuoka, Shizuoka 422-8526, Japan[1]; Department of Biological Sciences, University of Alberta, Edmonton, Alberta, Canada T6G 2E9[2]; and Department of Chemical and Materials Engineering, University of Alberta, Edmonton, Alberta, Canada T6G 2G6[3]

Received 8 July 2003/Accepted 29 September 2003

The mechanism of uptake of phenanthrene by *Mycobacterium* sp. strain RJGII-135, a polycyclic hydrocarbon-degrading bacterium, was examined with cultures grown on phenanthrene (induced for phenanthrene metabolism) and acetate (uninduced). Washed cells were suspended in aqueous solutions of [9-^{14}C]phenanthrene, and then the cells were collected by filtration. Low-level steady-state ^{14}C concentrations in uninduced cells were achieved within the first 15 s of incubation. This immediate uptake did not show saturation kinetics and was not susceptible to inhibitors of active transport, cyanide and carbonyl cyanide *m*-chlorophenylhydrazone. These results indicated that phenanthrene enters rapidly into the cells by passive diffusion. However, induced cells showed cumulative uptake over several minutes. The initial uptake rates followed saturation kinetics, with an apparent affinity constant (K_t) of 26 ± 3 nM (mean ± standard deviation). Uptake of phenanthrene by induced cells was strongly inhibited by the inhibitors. Analysis of cell-associated ^{14}C-labeled compounds revealed that the concurrent metabolism during uptake was rapid and was not saturated at the substrate concentrations tested, suggesting that the saturable uptake observed reflects membrane transport rather than intracellular metabolism. These results were consistent with the presence of a saturable, energy-dependent mechanism for transport of phenanthrene in induced cells. Moreover, the kinetic data for the cumulative uptake suggested that phenanthrene is specifically bound by induced cells, based on its saturation with an apparent dissociation constant (K_d) of 41 ± 21 nM (mean ± standard deviation). Given the low values of K_t and K_d, *Mycobacterium* sp. strain RJGII-135 may use a high-affinity transport system(s) to take up phenanthrene from the aqueous phase.

Many polycyclic aromatic hydrocarbons (PAHs) such as naphthalene, phenanthrene, fluoranthene, anthracene, pyrene, benz[*a*]anthracene, and benzo[*a*]pyrene are known to be utilized as sole carbon and energy sources, or are degraded cometabolically, by a diverse group of bacteria (11, 22). Biodegradation is a significant tool for the removal of these contaminants from environments, but their low bioavailability, especially for high-molecular-weight PAHs, has often been observed in the environment and bioremediation systems (2, 22). Due to their extremely hydrophobic nature, PAHs partition readily into solid and liquid organic phases and exist in aqueous phase only at limited concentrations. This makes uptake of PAHs by bacterial cells difficult. In bacterial cultures where only the compounds dissolved in aqueous solution are utilized, mass transfer or the rate of desorption controls the rates of degradation and culture growth (2).

Nevertheless, several studies have reported that degradation kinetics for the PAHs vary among different bacteria and that some bacteria apparently show rapid degradation of such PAHs with concomitant growth (16, 18, 37). Thus, some bacteria seem to have adapted to the low availability of PAHs. Mechanisms of the adaptation include the direct contact with solid-phase PAHs (4, 13, 38, 41) and biosurfactant excretion to facilitate desorption (15). Wick et al. (40, 41) have reported that the suspended cells of *Mycobacterium* sp. strain LB501T do not produce biosurfactant but have a strong ability to degrade low concentrations of aqueous-phase anthracene. The specific affinity (calculated as maximum degradation rate [V_{max}]/Michaelis-Menten half-saturation constant [K_m]) of LB501T cells for aqueous anthracene was found to be higher than the specific affinities of other cultures reported elsewhere (41). A diverse range of K_m values for PAH degradation have been obtained with pure cultures (1, 12, 18, 27, 36) and mixed cultures (19). Wick et al. have proposed the presence of a high-affinity uptake system in LB501T (41), which would account for the facile degradation of aqueous-phase PAHs occurring at extremely low concentrations in the environment. To explain such differences in the specific affinities or K_m values between species of bacteria, it seems reasonable to consider the roles of cell surface binding and membrane transport for aqueous PAHs as well as the affinity of intracellular enzymes responsible for PAH metabolism (10).

Only limited research has been carried out on the cellular binding and transport of PAHs in aqueous phase by bacteria. Bateman et al. (5) conducted uptake experiments with *Pseudomonas putida* PpG1064 by filtration of cells from naphthalene solutions and flow dialysis. Naphthalene was immediately sorbed into the cells and subjected to the intracellular metabolism. This uptake process did not show substrate saturation kinetics and was not susceptible to inhibitors such as cyanide and carbonyl cyanide *m*-chlorophenylhydrazone (CCCP), consistent with the lack of an active transport system in PpG1064 cells. Bugg et al. (9) demonstrated that *Pseudomonas fluore-*

* Corresponding author. Mailing address: Institute for Environmental Sciences, University of Shizuoka, 52-1 Yada, Shizuoka 422-8526, Japan. Phone: 8154-264-5649. Fax: 8154-264-5594. E-mail: miyatan@smail.u-shizuoka-ken.ac.jp.

scens LP6a transports phenanthrene, fluoranthene, and anthracene out of the cell by an active efflux mechanism. On the other hand, the influx depended upon passive diffusion that yielded a linear correlation between the octanol-water partition coefficients and LP6a cell-water partition coefficients for the tested PAHs (9). The results of these studies (5, 9) were consistent with a general view that the interior of the cytoplasmic membrane acts as a reservoir of hydrophobic compounds with high octanol-water partition coefficients (35). In contrast, incorporation of naphthalene by a specific, energy-dependent transport system was proposed in *P. fluorescens* Uper-1, based on reduction of uptake by inhibitors and the naphthalene analogue α-naphthol (39). The rates of naphthalene uptake were assessed mainly by monitoring substrate depletion in the supernatant of cell suspensions over 1 or 2 h. The Uper-1 cells degraded naphthalene extensively during incubation. Under these experimental conditions, the observed uptake may reflect metabolism and cell growth in addition to membrane transport. Thus, the conclusive evidence for the mechanism of bacterial PAH uptake has been confined to influx by passive diffusion. Given the diversity of PAH-utilizing bacteria and their different affinities for PAHs, however, the transport mechanism(s) described for a limited number of *Pseudomonas* strains may not be general.

Fast-growing *Mycobacterium* species, which belong to nocardioform actinomycetes, have often been isolated from contaminated soils and sediments by using high-molecular-weight PAHs as a carbon source (22). Because of their high ability to mineralize such PAHs, mycobacteria seem to play a role in the removal of PAHs from the environment. In this study, we examined the mechanism of uptake of aqueous-phase phenanthrene by *Mycobacterium* sp. strain RJGII-135, capable of degrading both low- and high-molecular-weight PAHs (17, 27, 33). The cell suspensions were prepared from cultures grown on either phenanthrene or acetate. The uptake experiments were conducted by incubation of suspended cells with [9-^{14}C]phenanthrene over several minutes. Phenanthrene was added at initial concentrations below the aqueous solubility limit. The hydrocarbon-exposed cells were separated by filtration, and the cellular ^{14}C accumulation was monitored and kinetically characterized. Concurrent metabolism during uptake was examined to elucidate the relative contributions of membrane transport and metabolism on the uptake of phenanthrene by *Mycobacterium* sp. strain RJGII-135.

MATERIALS AND METHODS

Chemicals. [9-^{14}C]phenanthrene (99% pure; 55 mCi mmol^{-1}) was obtained from American Radiolabeled Chemicals Inc. (St. Louis, Mo.). Nonlabeled phenanthrene (99% pure), naphthalene (99%), fluoranthene (97%), anthracene (98%), and pyrene (98%) were obtained from Wako Pure Chemical Industries (Osaka, Japan). These labeled and nonlabeled PAHs were dissolved in 99.5% ethanol for preparation of stock solutions. Another source of phenanthrene (95% pure; Wako Pure Chemical Industries) was used only for bacterial cultivation, not uptake studies. A mixture of phenanthrene *cis*-3,4- and *cis*-1,2-dihydrodiol isomers was produced in cultures of a transposon mutant (strain 11) of *P. fluorescens* LP6a, as previously described (14) and was isolated by thin-layer liquid chromatography (TLC) (34) using silica gel 60 F_{254} (Merck). The phenanthrene dihydrodiols were used as one representative of bacterial PAH metabolites. Potassium cyanide (Wako Pure Chemical Industries) and CCCP (Sigma-Aldrich Co.) were used as inhibitors of transport activity.

Organism, culture conditions, and preparation of cell suspension. *Mycobacterium* sp. strain RJGII-135 (17) was a generous gift from R. J. Grosser (U.S. Environmental Protection Agency, Cincinnati, Ohio) and maintained on Difco plate count agar at 8°C. MS medium (38) was modified and used as a basal medium: it contained (per liter) 0.8 g of KH_2PO_4, 1.2 g of K_2HPO_4, 0.5 g of NH_4Cl, 1.0 g of Na_2SO_4, 1.0 g of KNO_3, 0.2 g of $MgSO_4 \cdot 7H_2O$, 4 mg of $FeSO_4 \cdot 7H_2O$, and 1 ml of trace element solution (38), pH 7.0. To prepare complete medium, either sodium acetate (2 mmol) or solid phenanthrene (40 mg) was added to 100 ml of the liquid medium before autoclaving. Inoculum was grown on acetate for 4 days, and a portion (3 ml) was transferred into fresh medium containing solid phenanthrene or acetate, followed by incubation for 8 or 4 days, respectively. All incubations were conducted on a rotary shaker at 30°C. Both cultures were filtered through glass wool to remove solid phenanthrene and/or clumped cells. The optical densities at 600 nm (OD_{600}) of the filtrates containing suspended cells were approximately 0.15 and 0.5 when grown on phenanthrene and acetate, respectively. Cells were collected by centrifugation at 4,600 × *g* for 20 min and washed once with 0.1 M potassium phosphate buffer (pH 7.0) before the cells were resuspended at prescribed cell densities in the same buffer.

Phenanthrene degradation assay. The assay for degradation of phenanthrene started with the addition of 0.2 ml of a cell suspension (OD_{600} of 2.0) to glass test tubes containing a solution of nonlabeled phenanthrene dissolved at 5 μM in 2.0 ml of phosphate buffer (0.1 M, pH 7.0). Duplicate sets of incubations were conducted at room temperature with gentle shaking. Parallel cell-free controls were used for evaluation of abiotic loss of phenanthrene during the incubation and subsequent extraction. At timed intervals, 2.0 ml of *n*-hexane was added to the tubes capped with plastic closures having Teflon liners, and the contents were mixed by vortex for 1 min. Concentration of phenanthrene in the hexane extracts was monitored with a Shimadzu UV-1600 spectrophotometer at 252 nm (3). The hexane solution containing 5 μM phenanthrene gave an A_{252} of 0.32. The UV absorption spectrum at 220 to 400 nm was also monitored to ensure no interference by phenanthrene metabolites of the absorbance readings at 252 nm.

Uptake experiments. Uptake of phenanthrene by the RJGII-135 cells was assayed by the filtration method of Bateman et al. (5) but using Whatman GF/F glass fiber filters (pore size, 0.7 μm). Phenanthrene concentrations in assay mixtures were below the aqueous solubility limit (6.2 μM) (42). For uptake experiments, 20 μl of an ethanolic solution of [^{14}C]phenanthrene (plus nonlabeled phenanthrene) was added to glass test tubes containing 2.0 ml of phosphate buffer (0.1 M, pH 7.0). The tubes were incubated at 30°C for up to 40 min to completely dissolve phenanthrene in phosphate buffer. During the incubations, no significant loss of radioactivity due to volatilization of phenanthrene was observed. The uptake experiment started when 200 μl of a cell suspension was added at an OD_{600} of 0.01 or 0.1 to 0.2 (see below) to the test tubes at room temperature. At 15- or 30-s intervals over several minutes, 1.0 ml of sample was taken from each of the test tubes and applied to a GF/F filter under vacuum. The filters plus cells were washed once using 5 ml of phosphate buffer under vacuum for 30 s before being transferred into 10 ml of Scintisol EX-H (Dojin-do Laboratories, Kumamoto, Japan). The radioactivity was determined with an Aloka LSC-3100 liquid scintillation counter. The amount of phenanthrene adsorbed onto GF/F filter was determined by filtration of cell-free control assay mixtures. The ^{14}C adsorbed onto the filter usually accounted for <10% of the counts compared to when cell suspensions were loaded, so that this value was routinely subtracted from test filters to determine the cellular ^{14}C levels.

In some experiments, a stock solution of [^{14}C]phenanthrene was supplemented with nonlabeled anthracene, fluoranthene, or pyrene as well as nonlabeled phenanthrene. The concentration of these second PAHs in assay mixtures was 0.3 μM, corresponding to 76, 23, and 50% of the aqueous solubilities of anthracene, fluoranthene, and pyrene, respectively (42). Naphthalene at concentrations of 0.3 and 3.0 μM was also used as a second PAH, but it was added to assay mixtures just before the cell suspension was added, to reduce potential volatility losses.

In uptake experiments, care was taken with the cell density in assay mixtures to minimize the effect of substrate depletion during incubation. Phenanthrene-grown cells were added at an OD_{600} of 0.01 (2.4 μg of cell [dry weight] per ml), whereas acetate-grown cells were added at an OD_{600} of 0.1 to 0.2 (32 to 64 μg of cell per ml). At these cell densities, depletion of aqueous-phase phenanthrene during the incubations was less than 15% of the initial concentrations.

Kinetic analysis. The uptake of [^{14}C]phenanthrene added at concentrations of 0.03, 0.06, 0.11, 0.21, 0.28, and 0.51 μM was measured at 15-s intervals over at least 45 s. After confirming that the cumulative uptake proceeded linearly, an initial uptake rate was calculated by extrapolation to time zero. The apparent affinity constant (K_t) and the maximum velocity (V_{max}) were estimated by nonlinear regression analysis, based on the fit of the data to the Michaelis-Menten equation. The calculation was carried out with a Prism 3.0 software package (GraphPad Software Inc., San Diego, Calif.).

To examine whether phenanthrene is specifically bound to the RJGII-135

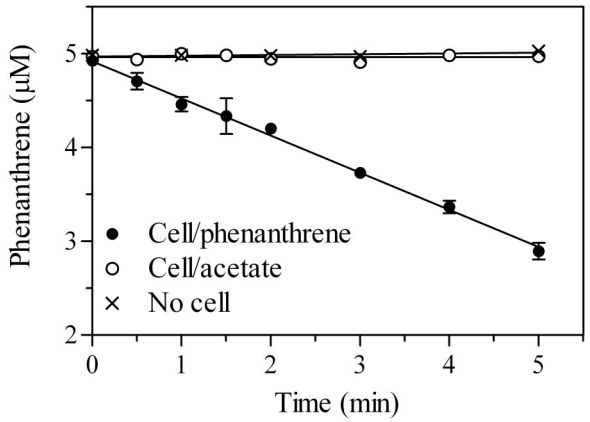

FIG. 1. Degradation of phenanthrene by suspended cells of *Mycobacterium* sp. strain RJGII-135 grown on either phenanthrene or acetate. Concentrations of residual phenanthrene in cultures were determined spectrophotometrically. Data points are means of duplicate measurements, and the error bars (where visible) represent 1 SD.

cells, the amounts of bound phenanthrene were estimated and plotted versus the initial aqueous concentrations. The data points were fitted to models for specific binding, nonspecific binding, and their combined mode. Specific binding of substrate is a saturable process and is generally given by the following equation: $b = B_{max} \cdot [S]/(K_d + [S])$, where b is the amount of specific binding, B_{max} is the maximum amount of specific binding, K_d is the equilibrium dissociation constant (substrate concentration yielding 1/2 B_{max}), and $[S]$ is the initial substrate concentration. Since nonspecific binding of substrate (referring to linear partitioning) is directly proportional to $[S]$, the combined mode of specific and nonspecific binding (b') is expressed as follows:

$$b' = \frac{B_{max} \cdot [S]}{K_d + [S]} + N \cdot [S] \quad (1)$$

The kinetic parameters B_{max}, K_d, and N (a slope for nonspecific binding) were estimated by nonlinear regression analysis using the Prism 3.0 software package.

Analysis of concurrent metabolism. For identification of the radiolabeled compounds in cells, the uptake experiment was conducted with a 10-fold volume of assay mixtures in 300-ml conical flasks. The cell suspension (2 ml) was added to 20 ml of phosphate buffer containing [^{14}C]phenanthrene at a prescribed concentration. Samples (10 ml) were taken at 45 or 60 s and filtered through Whatman GF/F glass fiber filters, and the filters were washed once with 5 ml of phosphate buffer. The total uptake of phenanthrene was determined by counting the radioactivity associated with the filters. In parallel experiments, the washed filters were immediately immersed in 2 ml of ethyl acetate and left overnight at room temperature. The filters were then further extracted three times in 2 ml of ethyl acetate. The extracts were pooled, and 0.5 ml of deionized water was added to remove debris liberated from the glass filter and cells. The water phase was combined with the filter, and these were transferred together into scintillation vials for determination of nonextractable (cell-bound) ^{14}C. The ethyl acetate phase was evaporated under a gentle stream of N_2 and redissolved in a small volume of acetone. The extracts in acetone were separated into two fractions of labeled compounds, phenanthrene and lipophilic metabolites, by TLC using silica gel 60 F_{254}. Benzene-hexane (1:1, vol/vol) was used as the developing solvent. In this solvent system, phenanthrene migrates toward the solvent front, and any metabolites remain around the origin on the plate (34). For detection of phenanthrene dihydrodiol, the extracts in acetone were also analyzed by TLC with the solvent benzene-ethanol (9:1, vol/vol) (34). Nonlabeled phenanthrene and *cis*-phenanthrene dihydrodiols were added to the radiolabel extracts and run simultaneously on TLC plates. The bands on the plate were visualized under UV light (254 nm), and radioactivity in the bands was counted in 10 ml of liquid scintillation fluid.

In separate experiments, the filters with cells were immersed in 2 ml of benzene–methanol–20% methanolic tetramethylammonium hydroxide (2:1:1, vol/vol/vol) and left overnight at 37°C, in order to disrupt the structure of mycobacterial cell envelope by alkaline methanolysis (28). The supernatant was collected, and the residue on the filter was washed three times in 2 ml of ethyl acetate. Deionized water (0.5 ml) was added to the combined supernatants to separate out hydrophilic compounds. The organic solvent phase was evaporated and the extracts were analyzed by TLC, as described above.

RESULTS

Degradation of phenanthrene by suspended cells. Cell suspensions of RJGII-135 obtained from cultures grown on acetate and phenanthrene were incubated with 5 μM phenanthrene, and degradation of phenanthrene was monitored spectrophotometrically at 252 nm (Fig. 1). The hexane extracts from all the incubation mixtures showed a UV absorption spectrum equivalent to that of authentic phenanthrene in hexane (λ_{max} = 251, 274, 281, and 292 nm), indicating that the A_{252} values represent only the concentrations of remaining phenanthrene. Figure 1 clearly shows that phenanthrene-grown cells are induced for phenanthrene metabolism, whereas acetate-grown cells are not.

Uptake of phenanthrene. When acetate-grown cells were incubated with 0.06 μM [^{14}C]phenanthrene, cellular ^{14}C reached a steady state by the time of the first sample at 15 s (Fig. 2A). If this immediate uptake includes a substrate-saturable process, addition of excess nonlabeled phenanthrene

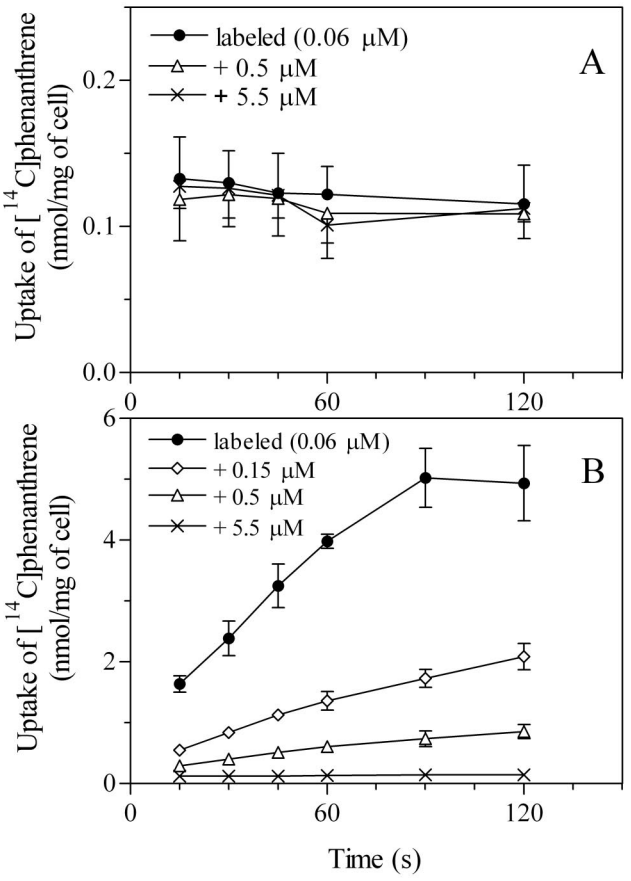

FIG. 2. Uptake of [^{14}C]phenanthrene by cells of *Mycobacterium* sp. strain RJGII-135 grown on acetate (A) or phenanthrene (B). Cells were incubated with 0.06 μM radiolabeled phenanthrene alone and with 0.06 μM radiolabeled phenanthrene plus 0.15, 0.5, or 5.5 μM nonlabeled phenanthrene. The error bars (where visible) represent 1 SD, based on three independent experiments.

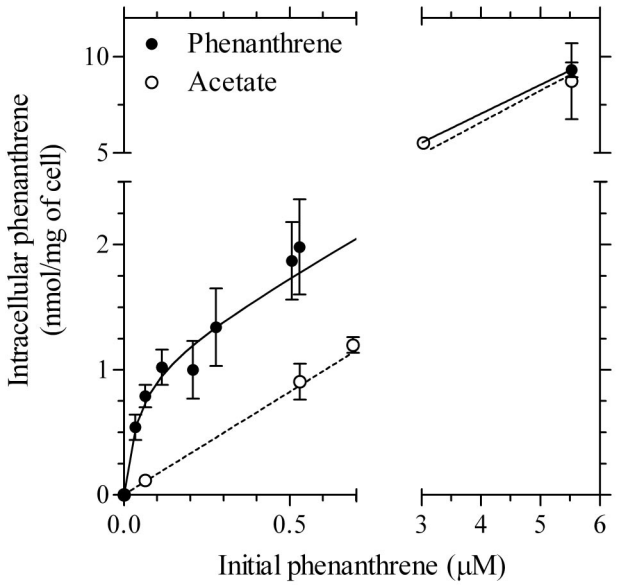

FIG. 3. Relationship between phenanthrene concentrations in cells of *Mycobacterium* sp. strain RJGII-135 and initial phenanthrene concentrations in aqueous phase. For phenanthrene-grown cells, the intracellular concentrations at time zero in Fig. 2 were estimated (see the text). For acetate-grown cells, the cellular steady-state concentrations were used. The solid line shows the nonlinear regression of the data for phenanthrene-grown cells to equation 1 with kinetic parameters K_d = 41 ± 21 nM, B_{max} = 1.1 ± 0.1 nmol mg of cell^{-1}, and N = 1.50 ± 0.04. The dashed line shows the linear regression of the data for the acetate-grown cells, with a slope for nonspecific binding of N = 1.65 ± 0.04. The error bars (where visible) represent 1 SD.

would result in a decrease in the cellular ^{14}C due to competition with radiolabeled phenanthrene. No significant decrease was obtained even when nonlabeled phenanthrene was present in about 100-fold excess (Fig. 2A). This result suggests that entry of phenanthrene into acetate-grown cells depends upon a nonsaturable, linear partitioning process (for the kinetics, see Fig. 3).

In contrast, the ^{14}C uptake by phenanthrene-grown cells was inhibited by excess nonlabeled phenanthrene (Fig. 2B). When the cells were incubated with 0.06 μM labeled phenanthrene, cellular ^{14}C increased linearly between 15 and 60 s and reached a steady state after 90 s. The amount of cellular ^{14}C at 90 s was 5.0 ± 0.5 nmol mg of cell^{-1} (mean ± standard deviation [SD]), which was about 40 times that of acetate-grown cells (Fig. 2A). The cumulative uptake of ^{14}C was also observed in the presence of excess nonlabeled phenanthrene (Fig. 2B). However, the cellular ^{14}C decreased gradually as the concentration of nonlabeled phenanthrene increased up to 5.5 μM. For example, addition of nonlabeled phenanthrene at 0.15, 0.5, and 5.5 μM reduced the cellular ^{14}C level at 45 s by 65, 86, and 96%, respectively. To study the effect of second PAHs, nonlabeled naphthalene, anthracene, fluoranthene, and pyrene were added, and the cellular ^{14}C levels were compared at the incubation time of 45 s. Addition of naphthalene at 0.3 and 3.0 μM reduced the ^{14}C level slightly to 94% ± 1% and 78% ± 5% (means ± SD; n = 3) of the value for control cells with 0.06 μM phenanthrene only. Addition of more phenanthrene at 0.3 μM reduced the uptake to 16% ± 0% of the original value, while anthracene, fluoranthene, and pyrene (each 0.3 μM) reduced the ^{14}C level to 48% ± 3%, 46% ± 4%, and 43% ± 10% of the control, respectively.

Kinetics of phenanthrene uptake. In Fig. 2B, the slope of linear lines drawn for ^{14}C uptake between 15 and 60 s was regarded as the initial rate of phenanthrene uptake. Initial uptake rates were repeatedly measured with different phenanthrene concentrations, ranging from 0.03 to 0.51 μM. The rates followed Michaelis-Menten kinetics (24 data points; $r^2 > 0.99$) with an apparent K_t of 26 ± 3 nM and a V_{max} of 4.2 ± 0.1 nmol mg of cell^{-1} min^{-1} (means ± SD).

It should be noted that the linear slopes between 15 and 60 s (Fig. 2B) did not pass through a cellular phenanthrene concentration of zero when extrapolated to time zero. As shown for acetate-grown cells (Fig. 2A), such an immediate uptake achieved by 15 s would involve a partitioning process. However, the ^{14}C level estimated by extrapolation to time zero (0.84 ± 0.05 nmol mg^{-1}) decreased to 0.29 ± 0.03, 0.19 ± 0.01, and 0.12 ± 0.01 nmol mg^{-1} with the addition of nonlabeled phenanthrene at 0.15, 0.5, and 5.5 μM, respectively (Fig. 2B). Consequently, the immediate uptake also appeared to involve saturation kinetics. The estimated concentrations in the cells at time zero from repeated uptake experiments with different substrate concentrations are plotted in Fig. 3 versus the initial aqueous concentrations of phenanthrene. The total phenanthrene concentrations were calculated by multiplying the extrapolated ^{14}C concentrations at time zero (from Fig. 2 and other data sets) by the ratio of total phenanthrene to labeled phenanthrene. A model that represents a combined mode of specific and nonspecific interactions between one ligand and receptor, as indicated in equation 1, was consistent with the data. The kinetic parameters were as follows, with a goodness of fit (30 data points; $r^2 > 0.99$): the apparent K_d and B_{max} were 41 ± 21 nM and 1.1 ± 0.1 nmol mg of cell^{-1}, respectively (means ± SD). The slope for nonspecific binding (N) was 1.50 ± 0.04. Figure 3 also shows a linear regression of the data obtained with acetate-grown cells; the plots represent the steady-state concentrations in cells. The N value was 1.65 ± 0.04 (15 data points; $r^2 > 0.99$).

Concurrent metabolism during phenanthrene uptake. To study the concurrent metabolism of phenanthrene during uptake, the cellular ^{14}C-labeled compounds were extracted with ethyl acetate and analyzed by TLC (Table 1). The validity of this method was confirmed with acetate-grown cells that were not induced for phenanthrene metabolism (Fig. 1). The uninduced cells incubated with 0.31 μM [^{14}C]phenanthrene incorporated 0.38 nmol of ^{14}C mg of cell^{-1}, of which nonextractable (cell mass-incorporated) compounds and lipophilic metabolites accounted only for <0.1 and 2%, respectively. This result clearly indicates that almost all the accumulated phenanthrene remained without being metabolized, consistent with the result of the degradation assay (Fig. 1). Due to its volatilization during evaporation of organic solvent, the recovery of phenanthrene after TLC analysis was somewhat lower (72%) than that expected from a material balance (98%) (Table 1).

To avoid underestimation of residual phenanthrene, the value calculated from material balance was used for considering to what extent phenanthrene was metabolized by the cells grown on phenanthrene. The phenanthrene-grown cells incubated with 0.06 μM [^{14}C]phenanthrene for 45 s accumulated

TABLE 1. Metabolism of phenanthrene incorporated into cells of *Mycobacterium* sp. strain RJGI1-135 grown on acetate or phenanthrene[a]

Cells and [^{14}C]phenanthrene concn (μM)	Total uptake (nmol of ^{14}C mg of cell^{-1})	^{14}C-labeled compound (% of total uptake)[b]		
		Nonextractable (cell bound)	Lipophilic metabolites	Phenanthrene
Acetate grown				
0.31	0.38 ± 0.04	<0.1	2.1 ± 0.3	98 (72 ± 1)
Phenanthrene grown				
0.06	2.8 ± 0.0	62 ± 2	10 ± 1	28 (<0.1)
0.18	4.8 ± 0.2	75 ± 4	21 ± 0	4 (1.0 ± 0.5)

[a] Phenanthrene-grown and acetate-grown cells were incubated with [^{14}C]phenanthrene for 60 and 45 s, respectively. Data are means ± SDs of two measurements.
[b] Intracellular labeled compounds were separated into three fractions: ethyl acetate-nonextractable (cell-bound) compounds, lipophilic metabolites, and residual phenanthrene. For phenanthrene amounts, estimated values from a material balance with the nonextractable and lipophilic fractions are shown; actual measurements by TLC are shown in parentheses.

2.8 nmol of ^{14}C mg^{-1}, of which nonextractable compounds, lipophilic metabolites, and residual phenanthrene accounted for 62, 10, and 28%, respectively (Table 1). When the concentration of [^{14}C]phenanthrene increased to 0.18 μM, the fractions of nonextractable compounds and lipophilic metabolites increased to 75 and 21%, respectively. The residual phenanthrene was estimated by material balance to be at most 4% of the total amount. One class of lipophilic metabolite, phenanthrene dihydrodiol(s), was detected at 2.2% ± 0.5% of total ^{14}C-labeled compounds (not shown in Table 1). It was unlikely that phenanthrene was sorbed deeply into the cell compartment; therefore, it would not likely contribute significantly to the fraction of nonextractable compounds. This interpretation was demonstrated by TLC analysis of the alkaline methanolysate of the cells that were incubated with 0.18 μM labeled phenanthrene for 45 s. The nonextractable compounds, hydrophilic (water-phase) metabolites, lipophilic metabolites, and residual phenanthrene accounted for 4.1% ± 0.4%, 93% ± 2%, 8.2% ± 0.9%, and 0%, respectively, of the total ^{14}C-labeled compounds (4.3 ± 0.2 nmol mg^{-1}) (means ± SD; n = 2). Thus, virtually all the cellular ^{14}C in phenanthrene-grown cells was present in the form of metabolites. These results indicate the occurrence of a rapid metabolism of phenanthrene during the uptake by phenanthrene-grown cells.

Effect of inhibitors on phenanthrene uptake. To study the energy-dependent uptake of phenanthrene, the effects of cyanide and CCCP (an uncoupler) on the cellular accumulation of ^{14}C were examined. Figure 4 shows one representative result of the inhibition assays with phenanthrene-grown cells. Cumulative phenanthrene uptake was completely inhibited by addition of cyanide (10 mM) at the beginning of incubation. The immediate uptake process achieved within the first 15 s was not susceptible to the inhibitor, because the ^{14}C concentration in unexposed cells at time zero (y intercept, 1.3 nmol mg of cell^{-1}) approximates the steady-state concentration observed for the cells initially exposed to cyanide (1.5 nmol mg^{-1}). CCCP (0.1 mM) showed equivalent effects, although the cumulative uptake proceeded slightly after the addition at the beginning of incubation. Addition of the two inhibitors at 45 s also strongly prevented the cumulative uptake but did not result in a further decrease in the cellular ^{14}C. This result indicates the lack of exodus of the accumulated ^{14}C. Neither cyanide nor CCCP affected phenanthrene uptake by acetate-grown cells (data not shown).

DISCUSSION

The mechanism of phenanthrene uptake by *Mycobacterium* sp. stain RJGII-135 was examined with cells that were induced (phenanthrene grown) and uninduced (acetate grown) for phenanthrene metabolism. In uninduced cells, steady-state concentrations of cellular phenanthrene were achieved within the initial 15 s of incubation. The lack of saturation and the lack of inhibition by azide and CCCP support the finding that this immediate uptake is caused by passive diffusion. Similar results have been reported for uptake of naphthalene by *P. putida* PpG1064 (5) and uptake of naphthalene, phenanthrene, anthracene, and fluoranthene by *P. fluorescens* LP6a (9). Steady-state PAH concentrations in cells of PpG1064 and LP6a were achieved by the times (10 s and 1 to 2 min, respectively) that the first samples were taken from incubation mixtures (5, 9). These observations suggest that, despite the large differences in the cell envelope structures between gram-negative and -positive bacteria, partitioning of PAHs into bacterial cell components occurs very quickly.

However, the induced cells showed a cumulative uptake curve over a period of a few minutes when incubated with [^{14}C]phenanthrene. Since phenanthrene enters immediately

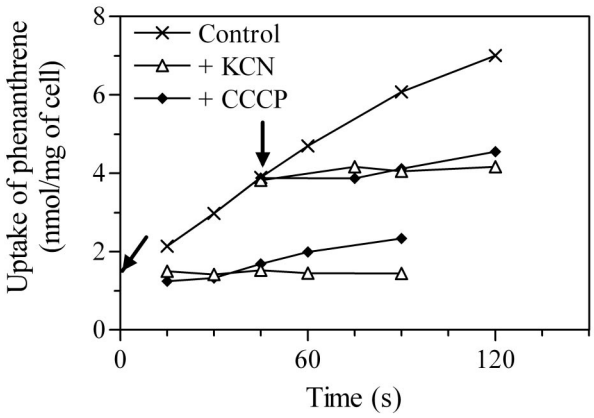

FIG. 4. Effect of inhibitors on uptake of phenanthrene by cells of *Mycobacterium* sp. strain RJGII-135 grown on phenanthrene. Cyanide (10 mM) or CCCP (0.1 mM) was added at time zero or at 45 s during incubation. The times when inhibitors were added are indicated with arrows.

into uninduced cells by passive diffusion, the continued cumulative uptake in induced cells must also involve a constant role of partitioning. Kinetic analysis revealed that linear partitioning is not the only mechanism that explains the immediate uptake in induced cells and suggests that phenanthrene is specifically bound to induced cells, based on the saturation kinetics (apparent $K_d = 41 \pm 21$ nM). The contribution of nonspecific binding, referred to as linear partitioning, had an N of 1.50 $\pm$ 0.04. The fair agreement between the two N values for induced and uninduced cells indicates that phenanthrene enters equivalently into both types of cells by passive diffusion. This suggests that induced cells accumulate additional phenanthrene by the phenomenon of specific binding. The kinetics described here for induced cells may be a conservative estimate of [^{14}C]phenanthrene uptake, since the induced cells used in uptake experiments likely contained residual cell-associated phenanthrene from their growth on nonlabeled phenanthrene; due to its competitive effect, this would reduce the apparent extent of uptake for labeled phenanthrene.

The data presented here are also consistent with the presence of a saturable, energy-dependent system in the cumulative uptake observed in induced cells. The uptake rates showed saturation kinetics (apparent $K_t = 26 \pm 3$ nM) and were largely reduced by the inhibitors. This K_t value is much smaller than that reported for the naphthalene uptake by *P. fluorescens* Uper-1 (11 μM) (39), suggesting the presence of a high-affinity uptake system in RJGII-135. Besides nonlabeled phenanthrene, the cumulative uptake of [^{14}C]phenanthrene responded to nonlabeled naphthalene, anthracene, fluoranthene, and pyrene to different extents. Since three- and four-ring PAHs inhibited the ^{14}C uptake more than two-ring PAH, the phenanthrene uptake system may have selectivity for larger PAHs.

The phenanthrene-grown RJGII-135 cells were induced for the phenanthrene metabolism. In such cells, the concurrent intracellular metabolism dissipates the equilibrium partitioning of a hydrophobic compound between cytoplasmic membrane and cytoplasm, so the metabolism rather than membrane transport might be a rate-determining step in the substrate influx. Also, since cyanide and CCCP may be potent inhibitors for the PAH-metabolic enzymes, they might inhibit the phenanthrene uptake by directly affecting the metabolic process. However, these assumptions were inconsistent with our data (Table 1). Analysis of the concurrent metabolism revealed that neither phenanthrene nor phenanthrene dihydrodiol(s) accumulated in cells that were incubated with 0.18 μM [^{14}C]phenanthrene. This result indicates that the intracellular metabolism is fast enough to maintain a low intracellular concentration of free phenanthrene. Also, the occurrence of rapid metabolism is partly explained by the fact that no cellular ^{14}C was excreted after addition of the inhibitors (Fig. 4). If phenanthrene was present in the cells without being metabolized, the inhibitor addition would result in the efflux of cellular [^{14}C]phenanthrene that accumulated beyond the level due to passive diffusion. Thus, the concurrent metabolism is not saturated at the substrate concentrations below 0.18 μM, where the uptake rate reaches approximately 90% of V_{max} given its K_t value. This observation shows that the concurrent metabolism is not a rate-determining step for the cumulative uptake process in induced cells. The result suggests that the cumulative uptake reflects the membrane transport rather than intracellular metabolism, although the possibility of contribution of metabolism cannot be ruled out. While PAH transport systems in *Pseudomonas* spp. have been reported previously (5, 9, 39), this study presents the first indications for the presence of a saturable, energy-dependent system for PAH transport in mycobacteria as well as the first possible involvement of specific binding of PAH to bacterial cells. It is not clear whether these two processes act in concert for the uptake of phenanthrene by RJGII-135, although these characteristics coexisted in the induced cells but not in uninduced cells.

Our kinetic data suggest that both passive diffusion and saturable transport system(s) contribute to the utilization of phenanthrene by RJGII-135. The culture medium, as well as other media generally used for liquid cultures of PAH-degrading organisms, was supplemented with solid phenanthrene at a concentration (0.4 g liter^{-1} in this study) far greater than the aqueous solubility limit. In such cases, mass transfer of phenanthrene to aqueous solution readily occurs until the maximum solubility. The results in Fig. 3 imply that at around the solubility limit, the mechanism of nonspecific binding dominates the immediate uptake in induced cells. The role of passive diffusion undoubtedly would be significant in the cultures of RJGII-135 with solid phenanthrene, as reported for two *Pseudomonas* strains (5, 9). Extensive research has demonstrated that heterologous expression of genes encoding PAH-metabolizing enzymes of various bacteria (e.g., species of *Pseudomonas* [26], *Nocardioides* [32], and *Mycobacterium* [24]) provides the host organisms such as *Escherichia coli* with the capability to degrade naphthalene, phenanthrene, or pyrene added in excess solid. Consequently, there is no requirement of an additional transport system for degradation of such PAHs by the host cells. In contrast, the results in Fig. 3 also imply that the contribution of specific (saturable) binding to the immediate uptake increases gradually with a decrease in the aqueous phenanthrene concentration. At a concentration of 0.06 μM, for example, the amount of phenanthrene specifically bound can be predicted to account for 88% of the total immediate uptake. Taken together with the K_t value for the subsequent cumulative uptake, the two saturable processes (i.e., binding and transport) in induced cells apparently respond to nanomolar levels of aqueous-phase phenanthrene. In this regard, their function(s) may be involved particularly in facilitated degradation of aqueous-phase phenanthrene occurring only at limited concentrations in environments, where hydrophobic compounds are partitioned into organic phases and the mass transfer or desorption proceeds only at limited rates (8, 16, 31). Recent studies have proposed the presence of facilitated or active transport systems for uptake of hydrophobic compounds: toluene (21) and *m*-xylene (23), alkanes such as *n*-hexadecane (6, 25, 30), and dibenzothiophene (29). Moreover, some long-chain fatty acids such as oleic acid are also known to be bound to bacterial cells and transported actively (7, 20). The roles of membrane transport and also specific binding in microbial degradation of PAHs with a limited bioavailability have been considered very little as yet, but the present study suggests that these mechanisms may contribute.

ACKNOWLEDGMENTS

We thank R. J. Grosser for providing *Mycobacterium* sp. strain RJGII-135 and T. Bugg for assistance in part of the experimental work.

This work was supported by Grant-in-Aid for Young Scientist (B) (14780445) from the Japan Society for the Promotion of Science.

REFERENCES

1. **Ahn, I.-S., W. C. Ghiorse, L. W. Lion, and M. L. Shuler.** 1998. Growth kinetics of *Pseudomonas putida* G7 on naphthalene and occurrence of naphthalene toxicity during nutrient deprivation. Biotechnol. Bioeng. **59:**587–594.
2. **Alexander, M.** 1999. Biodegradation and bioremediation, 2nd ed. Academic Press, San Diego, Calif.
3. **Barkay, T., S. Navon-Venezia, E. Z. Ron, and E. Rosenberg.** 1999. Enhancement of solubilization and biodegradation of polyaromatic hydrocarbons by the bioemulsifier alasan. Appl. Environ. Microbiol. **65:**2697–2702.
4. **Bastiaens, L., D. Springael, P. Wattiau, H. Harms, R. de Wachter, H. Verachtert, and L. Diels.** 2000. Isolation of adherent polycyclic aromatic hydrocarbon (PAH)-degrading bacteria using PAH-sorbing carriers. Appl. Environ. Microbiol. **66:**1834–1843.
5. **Bateman, J. N., B. Speer, L. Feduik, and R. A. Hartline.** 1986. Naphthalene association and uptake in *Pseudomonas putida.* J. Bacteriol. **166:**155–161.
6. **Beal, R., and W. B. Betts.** 2000. Role of rhamnolipid biosurfactants in the uptake and mineralization of hexadecane in *Pseudomonas aeruginosa.* J. Appl. Microbiol. **89:**158–168.
7. **Black, P. N., and C. C. DiRusso.** 1994. Molecular and biochemical analyses of fatty acid transport, metabolism, and gene regulation in *Escherichia coli.* Biochim. Biophys. Acta. **1210:**123–145.
8. **Brusseau, M. L., R. E. Jessup, and P. S. C. Rao.** 1991. Nonequilibrium sorption of organic chemicals: elucidation of rate-limiting processes. Environ. Sci. Technol. **25:**134–142.
9. **Bugg, T., J. M. Foght, M. A. Pickard, and M. R. Gray.** 2000. Uptake and active efflux of polycyclic aromatic hydrocarbons by *Pseudomonas fluorescens* LP6a. Appl. Environ. Microbiol. **66:**5387–5392.
10. **Button, D. K.** 1985. Kinetics of nutrient-limited transport and microbial growth. Microbiol. Rev. **49:**270–297.
11. **Cerniglia, C. E.** 1992. Biodegradation of polycyclic aromatic hydrocarbons. Biodegradation **3:**351–368.
12. **Dean-Ross, D., J. Moody, and C. E. Cerniglia.** 2002. Utilization of mixtures of polycyclic aromatic hydrocarbons by bacteria isolated from contaminated sediment. FEMS Microbiol. Ecol. **41:**1–7.
13. **Eriksson, M., G. Dalhammar, and W. W. Mohn.** 2002. Bacterial growth and biofilm production on pyrene. FEMS Microbiol. Ecol. **40:**21–27.
14. **Foght, J. M., and D. W. S. Westlake.** 1996. Transposon and spontaneous deletion mutants of plasmid-borne genes encoding polycyclic aromatic hydrocarbon degradation by a strain of *Pseudomonas fluorescens.* Biodegradation **7:**353–366.
15. **García-Junco, M., E. de Olmedo, and J.-J. Ortega-Calvo.** 2001. Bioavailability of solid and non-aqueous phase liquid (NAPL)-dissolved phenanthrene to the biosurfactant-producing bacterium *Pseudomonas aeruginosa* 19SJ. Environ. Microbiol. **3:**561–569.
16. **Grosser, R. J., M. Friedrich, D. M. Ward, and W. P. Inskeep.** 2000. Effect of model sorptive phases on phenanthrene biodegradation: different enrichment conditions influence bioavailability and selection of phenanthrene-degrading isolates. Appl. Environ. Microbiol. **66:**2695–2702.
17. **Grosser, R. J., D. Warshawsky, and J. R. Vestal.** 1991. Indigenous and enhanced mineralization of pyrene, benzo[*a*]pyrene, and carbazole in soils. Appl. Environ. Microbiol. **57:**3462–3469.
18. **Guerin, W. F., and S. A. Boyd.** 1992. Differential bioavailability of soil-sorbed naphthalene to two bacterial species. Appl. Environ. Microbiol. **58:**1142–1152.
19. **Guha, S., C. A. Peters, and P. R. Jaffé.** 1999. Multisubstrate biodegradation kinetics of naphthalene, phenanthrene, and pyrene mixtures. Biotechnol. Bioeng. **65:**491–499.
20. **Hirsch, D., A. Stahl, and H. F. Lodish.** 1998. A family of fatty acid transporters conserved from mycobacterium to man. Proc. Natl. Acad. Sci. USA **95:**8625–8629.
21. **Kahng, H.-Y., A. M. Byrne, R. H. Olsen, and J. J. Kukor.** 2000. Characterization and role of *tbuX* in utilization of toluene by *Ralstonia pickettii* PKO1. J. Bacteriol. **182:**1232–1242.
22. **Kanaly, R. A., and S. Harayama.** 2000. Biodegradation of high-molecular-weight polycyclic aromatic hydrocarbons by bacteria. J. Bacteriol. **182:**2059–2067.
23. **Kasai, Y., J. Inoue, and S. Harayama.** 2001. The TOL plasmid pWW0 *xylN* gene product from *Pseudomonas putida* is involved in *m*-xylene uptake. J. Bacteriol. **183:**6662–6666.
24. **Khan, A. A., R.-F. Wang, W.-W. Cao, D. R. Doerge, D. Wennerstrom, and C. E. Cerniglia.** 2001. Molecular cloning, nucleotide sequence, and expression of genes encoding a polycyclic aromatic ring dioxygenase from *Mycobacterium* sp. strain PYR-1. Appl. Environ. Microbiol. **67:**3577–3585.
25. **Kim, I. S., J. M. Foght, and M. R. Gray.** 2002. Selective transport and accumulation of alkanes by *Rhodococcus erythropolis* S+14He. Biotechnol. Bioeng. **80:**650–659.
26. **Kurkela, S., H. Lehväslaiho, E. T. Palva, and T. H. Teeri.** 1988. Cloning, nucleotide sequence and characterization of genes encoding naphthalene dioxygenase of *Pseudomonas putida* strain NCIB9816. Gene **73:**355–362.
27. **McLellan, S. L., D. Warshawsky, and J. R. Shann.** 2002. The effect of polycyclic aromatic hydrocarbons on the degradation of benzo[*a*]pyrene by *Mycobacterium* sp. strain RJGII-135. Environ. Toxicol. Chem. **21:**253–259.
28. **Minnikin, D. E., S. M. Minnikin, I. G. Hutchinson, M. Goodfellow, and J. M. Grange.** 1984. Mycolic acid patterns of representative strains of *Mycobacterium fortuitum*, '*Mycobacterium peregrinum*' and *Mycobacterium smegmatis.* J. Gen. Microbiol. **130:**363–367.
29. **Noda, K.-I., K. Watanabe, and K. Maruhashi.** 2003. Isolation of the *Pseudomonas aeruginosa* gene affecting uptake of dibenzothiophene in *n*-tetradecane. J. Biosci. Bioeng. **95:**504–511.
30. **Noordman, W. H., and D. B. Janssen.** 2002. Rhamnolipid stimulates uptake of hydrophobic compounds by *Pseudomonas aeruginosa.* Appl. Environ. Microbiol. **68:**4502–4508.
31. **Pignatello, J. J., and B. Xing.** 1995. Mechanisms of slow sorption of organic chemicals to natural particles. Environ. Sci. Technol. **30:**1–11.
32. **Saito, A., T. Iwabuchi, and S. Harayama.** 2000. A novel phenanthrene dioxygenase from *Nocardioides* sp. strain KP7: expression in *Escherichia coli.* J. Bacteriol. **182:**2134–2141.
33. **Schneider, J., R. Grosser, K. Jayasimhulu, W. Xue, and D. Warshawsky.** 1996. Degradation of pyrene, benz[*a*]anthracene, and benzo[*a*]pyrene by *Mycobacterium* sp. strain RJGII-135, isolated from a former coal gasification site. Appl. Environ. Microbiol. **62:**13–19.
34. **Shuttleworth, K. L., and C. E. Cerniglia.** 1997. Practical methods for the isolation of polycyclic aromatic hydrocarbon (PAH)-degrading microorganisms and the determination of PAH mineralization and biodegradation intermediates, p. 766–775. *In* C. J. Hurst, G. R. Knudsen, M. J. McInerney, L. D. Stetzenbach, and M. V. Walter (ed.), Manual of environmental microbiology. ASM Press, Washington, D.C.
35. **Sikkema, J., J. A. M. de Bont, and B. Poolman.** 1995. Mechanisms of membrane toxicity of hydrocarbons. Microbiol. Rev. **59:**201–222.
36. **Stringfellow, W. T., and M. D. Aitken.** 1995. Competitive metabolism of naphthalene, methynaphthalenes, and fluorene by phenanthrene-degrading pseudomonads. Appl. Environ. Microbiol. **61:**357–362.
37. **Tang, W.-C., J. C. White, and M. Alexander.** 1998. Utilization of sorbed compounds by microorganisms specifically isolated for that purpose. Appl. Microbiol. Biotechnol. **49:**117–121.
38. **Tongpim, S., and M. A. Pickard.** 1996. Growth of *Rhodococcus* S1 on anthracene. Can. J. Microbiol. **42:**289–294.
39. **Whitman, B. E., D. R. Lueking, and J. R. Mihelcic.** 1998. Naphthalene uptake by a *Pseudomonas fluorescens* isolate. Can. J. Microbiol. **44:**1086–1093.
40. **Wick, L. Y., T. Colangelo, and H. Harms.** 2001. Kinetics of mass transfer-limited bacterial growth on solid PAHs. Environ. Sci. Technol. **35:**354–361.
41. **Wick, L. Y., A. Ruiz de Munain, and D. Springael.** 2002. Responses of *Mycobacterium* sp. LB501T to the low bioavailability of solid anthracene. Appl. Microbiol. Biotechnol. **58:**378–385.
42. **Yalkowsky, S. H., S. C. Valvani, and D. Mackay.** 1983. Estimation of the aqueous solubility of some aromatic coumpounds. Residue Rev. **85:**43–55.